Journal of Solid State Chemistry **168,** 474–485 (2002)
doi:10.1006/jssc.2002.9732

Molecular Complexes of Fullerenes C_{60} and C_{70} with Saturated Amines

D. V. Konarev,* A. Yu. Kovalevsky,† A. L. Litvinov,* N. V. Drichko,‡ B. P. Tarasov,* P. Coppens,† and R. N. Lyubovskaya*,[1]

*Institute of Problems of Chemical Physics, Chernogolovka, Moscow Region 142432, Russia; †Department of Chemistry, State University of New York at Buffalo, Buffalo, New York 14214; and ‡A.F. Ioffe Physical-Technical Institute, St.-Petersburg 194021, Russia

Received December 20, 2001; in revised form March 26, 2002; accepted April 10, 2002

New molecular complexes of fullerenes C_{60} and C_{70} with leuco crystal violet (LCV, 1–3); leucomalachite green (LMG, 4–6); crystal violet lactone (CVL, 7); *N*,*N*,*N*′,*N*′-tetrabenzyl-*p*-phenylenediamine (TBPDA, 8, and 9); *N*,*N*,*N*′,*N*′-tetramethyl-*p*-phenylenediamine (TMPDA, 10, and 11); triphenylamine (TPA, 12, and 13); and substituted phenotellurazines (EPTA and TMPTA, 14, and 15) have been synthesized. Crystal structures have been solved for C_{60} complexes with LMG (5, 6) TBPDA (8), TMPDA (10), and TPA (12). The C_{60} molecules form closely packed double layers in 5 and 6, hexagonal layers in 10 and quasi-three-dimensional layers in 8 and 12. The substitution of disordered solvent molecules in the complexes with LMG (4, 5) by naphthalene ones results in the ordering of the C_{60} molecules. According to IR-, UV–visible–NIR and ESR-spectroscopy the complexes have a neutral ground state. The spectra of 1–8, and 10 show intense charge transfer bands in the visible and NIR-range. On photoexcitation by white light (light-induced ESR (LESR) spectroscopy), 1 and 10 were shown to have an excited ionic state. The LESR signals were generated at light energies <2.25 eV indicating that the excited states in the complexes are realized mainly by direct charge transfer from donor to the C_{60} molecule. © 2002 Elsevier Science (USA)

Key Words: **fullerenes; molecular complexes; amines; structure; photoexcitation; charge transfer.**

INTRODUCTION

Great interest to fullerene-based compounds is attracted not only due to unusual conducting and magnetic properties of the C_{60} (1–3) salts, but possible photoinduced electron transfer (PIET) in neutral composites, dyad and triad molecules comprising fullerenes (4–6). Unique photoacceptor properties of fullerenes allow generation of relatively long-lived charge-separated states with high quantum yields under photoexcitation of conjugated polymers and other chromophore molecules in the presence of C_{60} (4–6). Molecular complexes of fullerenes with chromophore molecules of zinc tetraphenylporphyrin, (7, 8) bianthrone (9) and some amines (9) in the solid state may also be promising in the study of PIET. However, PIET in the fullerene complexes with amines has been studied up to now mainly in solutions (10–13).

Several fullerene complexes with amines were characterized in the solid state. They are ionic fullerene complexes with tetrakis(dimethylamino)ethylene (TDAE) and its analogs (2, 14), and neutral complexes of C_{60} with porphyrazine, (15) tetraphenylporphyrin, (16, 17) *N*,*N*,*N*′,*N*′-tetramethyl-*p*-phenylenediamine (TMPDA) (18), azotriptycene, (19) and 4-benzoyl-3-methyl-1-phenyl-2-pyrazoline-5-one (20).

The present work reports on the preparation of a series of new molecular complexes of C_{60} and C_{70} with substituted amines (see scheme 1). Crystal structures of five complexes together with IR, UV–visible–NIR- and ESR- spectra of the obtained compounds were studied. The dependencies of LESR signal intensity on photon energy was studied in **1** and **10** by LESR spectroscopy. The comparative analysis of these dependencies and the UV–visible spectra of the complexes allow one to assume the mechanism for PIET.

EXPERIMENTAL SECTION

Materials

All chemicals were purchased from Aldrich and Lancaster and used without further purification. Dry liquids were obtained by distillation under Ar over Na/benzophenone for benzene and P_2O_5 for chlorobenzene. The solvents were stored under argon.

Syntheses

All the complexes (Table 1) were obtained (50–80% yield) by evaporation of the solutions of fullerenes and

[1] To whom correspondence should be addressed. Fax: + 7 096 524 4401. E-mail: lyurn@icp.ac.ru.

0022-4596/02 $35.00

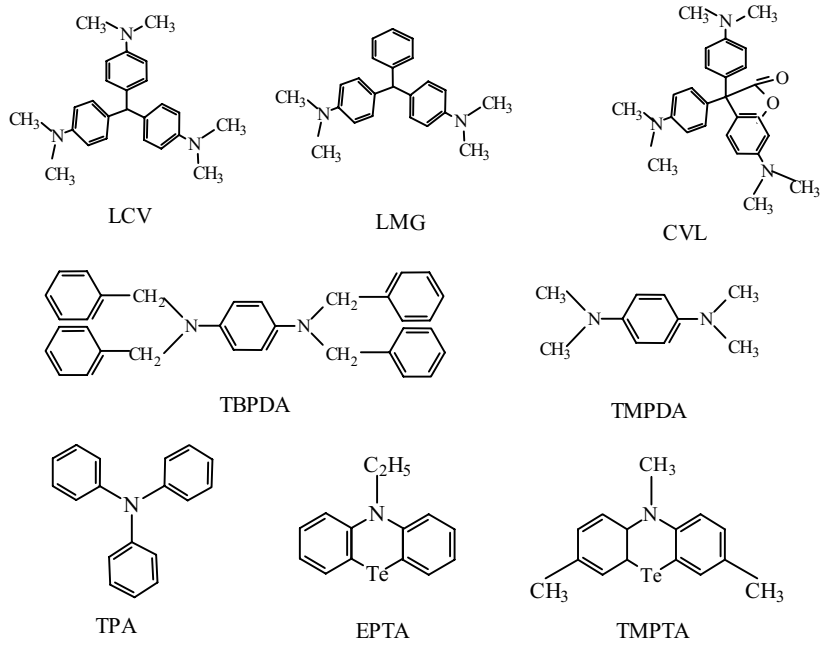

SCHEME 1. Molecular structures of the amines.

TABLE 1
The Data for Compounds 1–15

No.	Complex	Elemental analysis found/Calc.				TG-analysis, % (*T*, K)		
		C (%)	H (%)	N (%)	Cl (%)	Solvent	Donor	Shape of the crystals
1	LCV · C_{60} · C_6H_5Cl	Ref. [20]				5.6 (150)	4.7 (350)	Plates
2	LCV · C_{60} · C_6H_6	92.83	3.08	2.67	—	4.7	8	Plates
		93.50	3.14	3.36		(160)	(350)	
3	LCV · C_{70}	93.41	3.04	4.15	Abs.	—	—	Prisms
		93.33	2.83	3.84				
4	LMG · C_{60} · C_6H_6	94.61	3.00	2.26	—	2.2	12.5	Rhombus
		94.81	2.77	2.42		(120)	(350)	
5	LMG · C_{60} · $0.2C_7H_8$ · 0.3 · C_6H_5Cl	According to X-ray diffraction data				—	—	Parallelep.
6	LMG · C_{60} · $0.5C_{10}H_8$	According to X-ray diffraction data				—	—	Parallelep.
7	CVL · C_{60} · C_6H_6	93.20	3.31	3.13	—	3.2	7.8	Prisms
		91.03	2.88	3.46		(150)	(260)	
8	TBPDA · $2C_{60}$	According to X-ray diffraction analysis				—	—	Rhombus
9	TBPDA · C_{70}	95.32	2.22	2.28	Abs.	—	—	Elongated parallelep.
		95.42	2.44	2.14				
10	TMPDA · C_{60}	According to X-ray diffraction analysis				Abs.	12.6 (250)	Prisms
11	TMPDA · C_{70}			2.32	Abs.	Abs.	10.3	Prisms
				2.78			(250)	
12	TPA · C_{60}	According to X-ray diffraction analysis				—	—	Parallelep.
13	TPA · $2C_{60}$	96.84	1.14	0.85	—	Abs.	6	Elongated
		98.28	0.89	0.83			(215)	Parallelep.
14	EPTA · C_{60} · $0.2C_6H_5Cl$			1.17	0.68	—	—	Prisms
				1.30	0.66			
15	TMPTA · $2C_{60}$ · $2C_6H_5Cl$	88.95	2.07	0.8	3.20	—	—	Rhombus
		88.19	1.29	0.7	3.54			

Note. Abbreviations for donor compounds: LCV: Leuco Crystal Violet (4,4′, 4″-methylidynetris(*N*,*N*-dimethylaniline)); LMG: Leucomalachite Green (4,4′-benzylidene(*N*,*N*-dimethylaniline)); CVL: crystal violet lactone; TBPDA : *N*,*N*,*N*′,*N*′-tetrabenzyl-*p*-phenylenediamine; TPA: triphenylamine; EPTA: *N*-ethylphenotellurazine; TMPTA: 2,8, *N*-trimethylphenotellurazine. Abs.— absent, parallelep.—parallelepipeds.

corresponding amine under argon during 7–14 days. The solvent was decanted from the crystals before the precipitation of excesses of donor. The composition was determined by elemental and thermogravimetric analyses (**1–4**, **7**, **9–11**, **13–15**) and using X-ray diffraction data (**5**, **6**, **8**, **10**, and **12**).

The crystals of **1**, **3**, and **8–15** were obtained by evaporation of chlorobenzene solutions containing amine and C_{60} or C_{70} at a 10 (**1**), 20 (**3**), 3 (**8**), 5 (**9**), 30 (**10**), 100 (**11**), l0 (**13**), 8 (**14**), 8 (**15**) :1 molar ratio. The crystals of **12** were obtained as an admixture (with 10% yield) in the synthesis of **13**. The prisms of **12** were separated from the elongated parallelepipeds of **13** under microscope.

Complexes **2**, **4**, and **7** were obtained by evaporation of benzene solutions containing amine and C_{60} at a 20:1 molar ratio, **5** forms as an admixture in benzene (with 30% yield) in the synthesis of **4** in the presence of toluene and chlorobenzene vapors, **6** was obtained on evaporation of benzene solution containing $LMG:C_{10}H_8:C_{60} = 5:10:1$. Complex **4** is unstable in storage and decomposes to powder during 2 weeks due to the loss of the solvent, **5** and **6** are stable in storage.

General

IR spectra of the samples (in KBr pellets, 1:400) were recorded on a "Perkin Elmer 1725X" spectrophotometer in the 400–7000 cm^{-1} range. Electronic absorption spectra were recorded on a "Perkin Elmer Lambda 19 UV–vis–NIR" spectrophotometer in the 220–3000 nm range (KBr pellets, 1:2000).

A Bruker EMX (X-band) ESR spectrometer with an Oxford variable temperature cryostat (4–300 K operating range) was used. A xenon lamp connected to a monochromator (400–900 nm range) was used to excite the samples through a grid on the cavity. The samples were put into quartz tubes and the tubes were evacuated before measurements. We measured two types of spectra: the "dark" spectrum (the scan of the ESR spectrum of a non-illuminated sample) and then the "light on" spectrum (the scan of the ESR spectrum under light excitation). To discriminate the LESR signals we subtracted the "dark" spectrum from the "light on" one. To obtain the dependence of the LESR signals intensity on the photon energy, we normalized the integral intensity of the LESR signals on the light power and a number of photons.

Crystallographic data and parameters of the X-ray analysis for **5**, **6**, **8**, **10** and **12** are presented in Table 2. The X-ray diffraction data were collected at 90 K on a Bruker 1 K SMART CCD diffractometer equipped with a rotating anode (Mo$K\alpha$ radiation, $\lambda = 0.71073$ Å). The data were collected by the rotation method with a 0.3° frame width (ω scan). The data collection nominally covered full reciprocal space by a combination of six ω scans (600

TABLE 2
Crystal Data for 5, 6, 8, 10 and 12

Compound	**5**	**6**	**8**	**10**	**12**
Formula	$LMG \cdot C_{60} \cdot 0.2C_7H_8 \cdot 0.3C_6H_5Cl$	$LMG \cdot C_{60} \cdot 0.5C_{10}H_8$	$TBPDA \cdot 2C_{60}$	$TMPDA \cdot C_{60}$	$TPA \cdot C_{60}$
M_r (g/mol)	1100.13	1179.28	1909.82	884.85	965.91
Crystal system	Triclinic	Triclinic	Monoclinic	Monoclinic	Triclinic
Space group	*P*-1	*P*-1	*C*2/*m*	$P2_1/c$	*P*-1
a (Å)	12.9084(8)	13.0305(8)	23.208(3)	10.2811(7)	9.9044(6)
b (Å)	13.6615(9)	13.5964(8)	19.740(3)	17.225(1)	13.2877(8)
c (Å)	15.502(1)	15.499(1)	20.372(3)	10.2476(7)	16.2977(11)
α (deg)	77.694(1)	77.316(2)	90	90	76.898(1)
β (deg)	67.526(1)	67.238(2)	122.758(2)	101.930(2)	87.012(2)
γ (deg)	72.341(1)	72.286(2)	90	90	73.099(2)
V (Å^3)	2392.3(5)	72.286(2)	7849.0(2)	1775.6(2)	1998.6(2)
Z	2	2	8	2	2
ρ_{calc} (g/cm^3)	1.527	1.546	1.616	1.655	1.605
μ (mm^{-1})	0.10	0.089	0.09	0.096	0.09
T (K)	90.0(1)	90.0(1)	90.0(1)	90.0(1)	90.0(1)
Max. 2θ (deg)	56.8	58.6	55.1	59.5	63.2
Ref. measured	20,266	22,500	50,086	17,750	40,261
Unique ref.	10,292	11,069	8845	4512	12,056
(R_{int})	(0.036)	(0.077)	(0.090)	(0.092)	(0.062)
Ref. $I > 4\sigma(I)$	7344	5247	4410	2396	7324
Parameters refined	1149	816	778	328	1055
R [$I > 2\sigma(I)$]	0.054	0.046	0.082	0.055	0.055
WR_2	0.173	0.094	0.269	0.158	0.152
G.O.F.	0.978	0.796	1.035	0.981	1.016

Note. Ref.- reflection.

frames in each set), with different φ angles. Reflection intensities were integrated using SAINT program (21).

The solution and refinement of the structures were performed with SHELXTL program package (22). The structures were refined by full-matrix least squares against F^2 of all data. Non-hydrogen atoms were refined in anisotropic approximation. Hydrogen atoms were partially revealed from the difference Fourier maps and refined using ''riding'' model for aromatic H-atoms or in idealized positions for methyl H-atoms ($U_{iso} = 1.5U_{eq}$ of the preceding carbon atom for CH_3 hydrogens and $U_{iso} = 1.2U_{eq}$ for the rest H-atoms). Certain groups of atoms, namely atoms of disordered toluene and chlorobenzene in **5** were refined isotropically and applying bond length restraints (C_{ar}–C_{ar} 1.395(5) Å and C_{ar}–CH_3 1.450(5) Å). A disordered C_{60} molecule in **12** was refined with several bond length restrains (several C–C bonds restrained to have ideal values of 1.38(1) and 1.45(1) Å).

RESULTS AND DISCUSSION

Synthesis

Molecular complexes of fullerenes with various amines can be prepared by slow evaporation of a solvent containing fullerene and corresponding amine in argon atmosphere. In contrast to donors of other families (substituted tetrathiafulvalenes, aromatic hydrocarbons) (23), fullerene complexes with amines are formed only in the presence of large excesses of amines (fullerene:amine molar ratio up to 1:100). An important requirement to amine geometry in complex formation with fullerenes is their conformational flexibility or the presence of labile aryl substituents.

The resulting compounds and their characteristics are listed in Table 1. All the crystals are stable in storage except LMG · C_{60} · C_6H_6 (**4**), which decomposes due to the loss of solvent. Its preparation in the presence of toluene and chlorobenzene vapors or naphthalene yields the stable crystals of LMG · C_{60} · $0.2C_7H_8$ · $0.3C_6H_5Cl$ (**5**) and LMG · C_{60} · $0.5C_{10}H_8$ (**6**), respectively.

Crystal Structures

LMG · C_{60} · $0.2C_7H_8$ · $0.3C_6H_5Cl$ (5). C_{60}, and LMG reside at general positions. Toluene and chlorobenzene molecules (40/60% ratio, respectively) are at special positions and disordered by the inversion center located at the center of their benzene rings. The C_{60} molecules are also disordered between two orientations linked to each other by rotation of the C_{60} molecule about the six-fold axis which passes through the centers of two oppositely located hexagons with 65/35 occupancy. Figures 1 and 2 show only 65% of occupied orientation.

Complex **5** has a layered structure, in which double layers of the C_{60} molecules alternate with the layers consisting of the LMG ones along the *a*-axis (Fig. 1). The double layers of the C_{60} molecules are composed of zig-zag chains arranged along the *a*-axis. Each C_{60} molecule has four neighboring C_{60} ones. The two neighboring C_{60} molecules are located in the same chain and the other two ones in the adjacent chains with the distances between the centers of 9.84, 9.68 and 9.75, 9.63 Å, respectively. These distances are shorter than typical center-to-center distances in pure fullerene (9.95 Å at 150 K (24)), but essentially longer than a center-to-center distance in polymerized C_{60} phases (25) (9.26 Å). The close packing of the C_{60} molecules in **5** results in the formation of multiple shortened $C(C_{60})\ldots C(C_{60})$ van der Waals contacts (15 contacts for each C_{60} molecule in the 3.00–3.38 Å range).

The donor layers are composed of pairs of the LMG molecules (Fig. 1). Within the pairs, the C–H bond of one LMG molecule is directed to the center of a phenyl ring of another LMG molecule with a hydrogen-to-phenyl distance of 2.66 Å and an angle of 171°.

Each LMG molecule forms shortened van der Waals contacts with carbon atoms of two adjacent C_{60} molecules with the C···C distances in the 3.22–3.41 Å range (Fig. 2). There are also several shortened $N(LMG)\cdots C(C_{60})$ contacts in **5** in the 2.99–3.20 Å range. The disordered solvent molecules occupy the cavities between the layers of the C_{60} and LMG molecules without any shortened van der Waals contacts.

The dihedral angle between the $(CH_3)_2N$–C_6H_4– fragments of the LMG molecule in **5** is 77°, and those between the $(CH_3)_2N$–C_6H_4– fragment and the phenyl group are 66.4° and 59.4°. The nitrogen atoms of LMG have planar-trigonal conformation with the CH_3-groups in the plane of the –C_6H_4– fragment.

*LMG · C_{60} · $0.5C_{10}H_8$ (**6**).* Complex **6** is isostructural to **5** and contains naphthalene molecules instead of the disordered C_7H_8 and C_6H_5Cl ones in **5** (Fig. 3). LMG, naphthalene and C_{60} are ordered, with naphthalene residing at the inversion center.

*TBPDA · $2C_{60}$ (**8**).* The TBPDA and C_{60} molecules reside at special positions. One of the C_{60} molecules is disordered between two orientations linked by the non-crystallographic two-fold axis which passes through two oppositely located 6–6 bonds. Two orientations were refined with 60/40% of occupancies. Figure 4 shows only one orientation with the 60% occupancy.

Fullerenes form deformed puckered layers arranged along a diagonal to the *ac* plane (Fig. 4). Each C_{60} molecule has five neighboring C_{60} ones in the layer with the center-to-center distances of 9.77 (two distances), 10.10

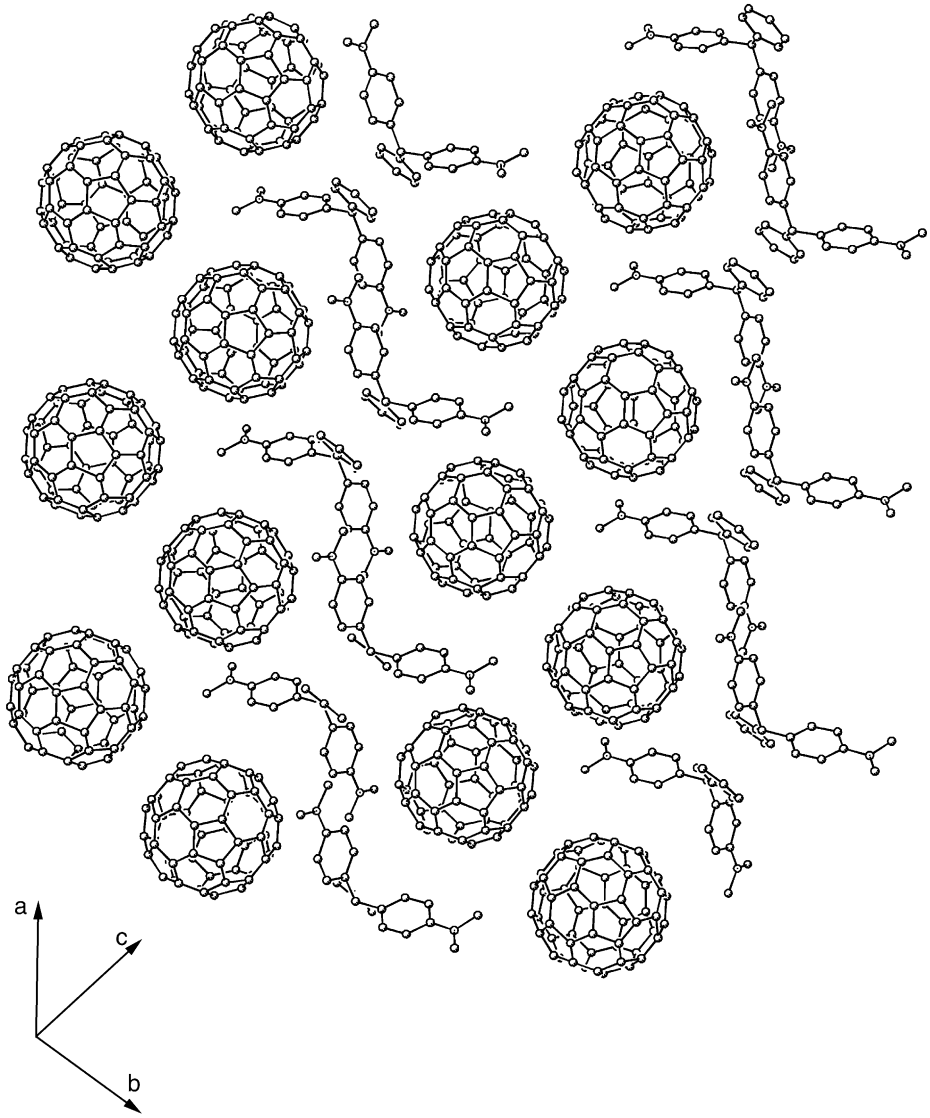

FIG. 1. The packing of the C_{60} and LMG molecules in LMG · C_{60} · 0.2C_7H_8 · 0.3 C_6H_5Cl (**5**). The layers composed of the C_{60} and LMG molecules alternate along the *a*-axis.

(two distances), and 10.67 Å (one distance), several of them being shorter than the van der Waals diameter of the C_{60} molecule (10.18 Å). Due to the strong puckering of the C_{60} layers, each C_{60} molecule also has two neighboring C_{60} ones from the adjacent layer with a center-to-center distance of 10.25 Å.

TBPDA molecules occupy cavities between the C_{60} layers (Fig. 4). There are two symmetrically independent TBPDA molecules in an asymmetric unit of **8**, which differ by the twisting angles of substituents at nitrogen atoms relatively to the central phenylene group.

TBPDA molecules (***I***) (Fig. 4) form van der Waals contacts only by phenyl groups with pentagons of C_{60} with the C···C distances in the 3.42–3.55 Å range. However, these fragments are positioned non-parallel to each other. The central phenylene group of TBPDA (***I***) arranges perpendicular to hexagons of the adjacent C_{60} molecules. TBPDA molecules (***II***) form short van der Waals contacts only by the central phenylene group with hexagons of the two C_{60} molecules. It should be noted that the TBPDA molecules of both types form several shortened H(TBPDA)···C(C_{60}) contacts in the 2.68–2.82 Å range which probably stabilize this structure. Geometry of the TBPDA molecules in **7** is similar to that in the TBPDA crystals (24).

TMPDA · *C_{60}* (**10**) has the same composition as reported previously for TMPDA · C_{60} (18). However, it has the triclinic unit cell instead of the monoclinic one[18].

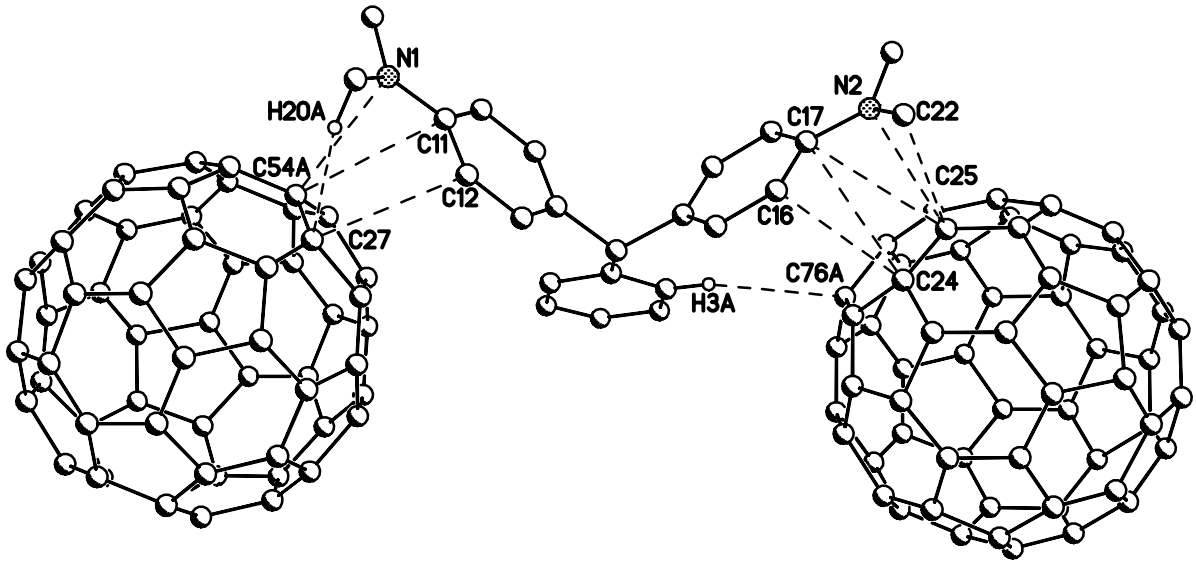

FIG. 2. Shortened van der Waals contacts between LMG and C_{60} molecules in LMG · C_{60} · $0.2C_7H_8$ · 0.3 C_6H_5Cl (**5**) (dotted lines).

This may be a new crystal modification of TMPDA · C_{60}. TMPDA and C_{60} are ordered and reside at general positions at the inversion center, with the asymmetric unit having halves of the molecules.

In the crystal, fullerene and donor molecules make alternating layers along the *c* axis (Fig. 5). In each C_{60} layer the fullerene molecule has six neighbors. The center-to-center distances between them are 10.02 (four distances)

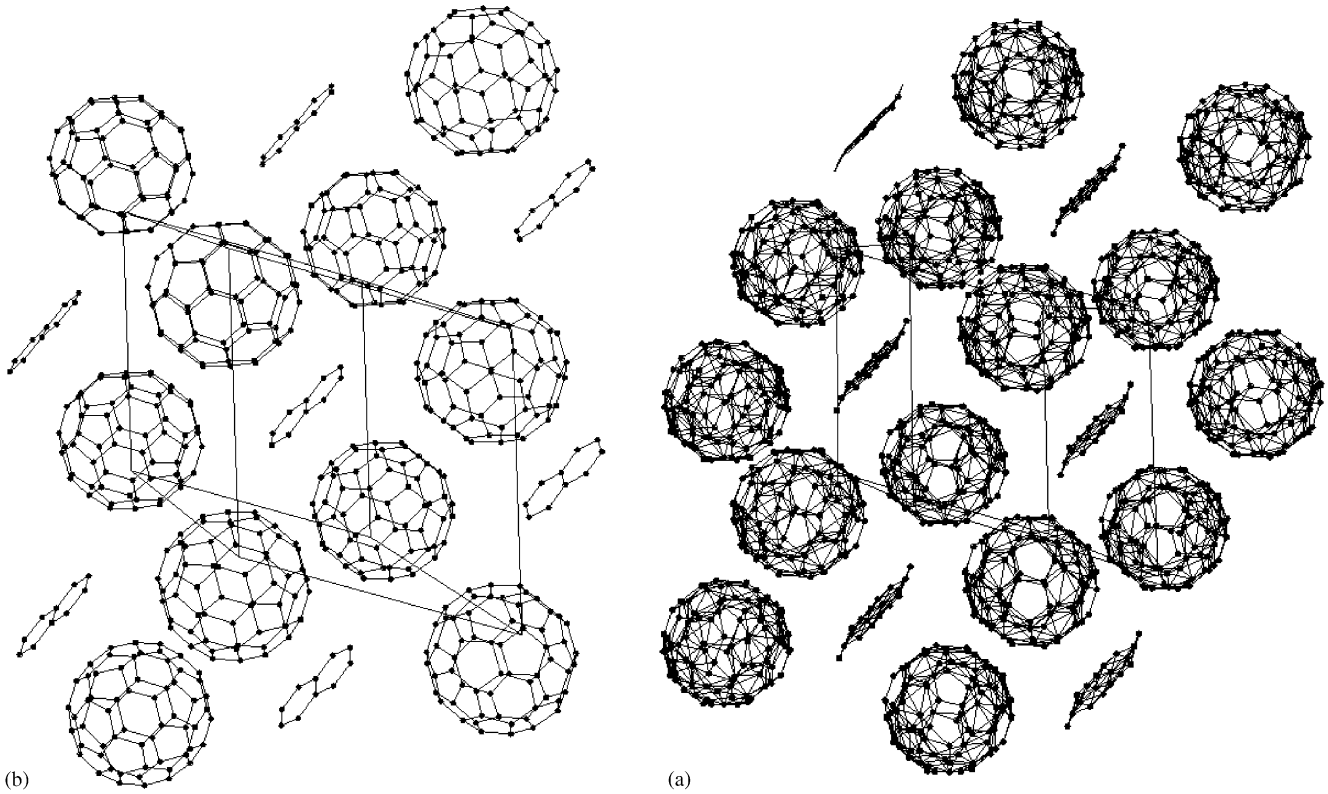

FIG. 3. The arrangement of the disordered C_{60} and C_7H_8, C_6H_5Cl molecules in **5** (a) and the ordered C_{60} and naphthalene molecules in **6** (b).

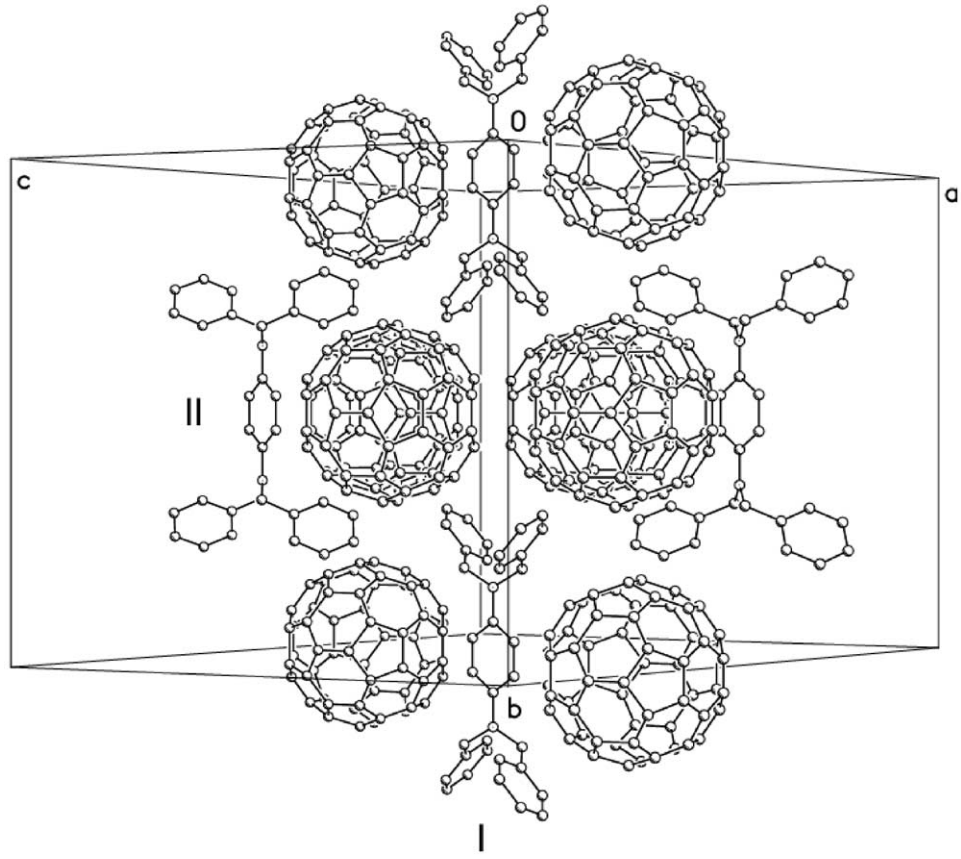

FIG. 4. Projection of crystal structure of TBPDA$(C_{60})_2$ (**8**) along the diagonal to the *ac* plane. Two types of TBPDA molecules are marked as **I** and **II**.

and 10.25 Å (two distances). This gives rise only to two shortened van der Waals contacts between them (3.38 and 3.41 Å).

Each TMPDA molecule forms shortened van der Waals contacts with four adjacent C_{60} spheres (Fig. 6). Two of these contacts are π–π interactions between benzene ring of TMPDA and 6–6 bonds of two fullerenes with the shortened C(TMPDA)$\cdots$C (C_{60}) van der Waals contacts in the 3.12–3.35 Å range. The other two contacts are H$\cdots\pi$ non-conventional hydrogen bonds between hydrogen atom of TMPDA and the six-membered ring of neighboring C_{60} (the H$\cdots\pi$ distance is 2.63 Å, the C–H$\cdots\pi$ angle is 151.1°).

The TMPDA molecule is almost planar. Nitrogen atom has planar-trigonal configuration. However, one of the methyl groups is slightly displaced from the molecule plane (the torsion angle is 167.5(2)°).

*TPA · C_{60} (**12**).* TPA and C_{60} molecules reside at general positions. The C_{60} molecules are disordered between two orientations linked by the non-crystallographic six-fold axis passing through the centers of two oppositely located hexagons. Two orientations were refined with 60/40% of occupancies. Fig. 7 shows only 60% of occupied orientation.

Crystal structure of **12** is layered. The distorted puckered C_{60} layers, which are similar to **8** arrange along a diagonal to the *bc* plane (Fig. 8). However, fullerene molecules in **12** are packed essentially denser than in **8**. Each C_{60} molecule has five neighboring ones in the layer with center-to-center distances of 9.90, 9.96 and 10.01 Å. All these distances are less than van der Waals diameter of the C_{60} molecule (10.18 Å). Due to the distortion of the layers each C_{60} molecule also has one neighbor from the adjacent layer with the center-to-center distance of 10.04 Å thus making the packing of the C_{60} molecules quasi-three dimensional.

The TPA molecules occupy the cavities between the distorted C_{60} layers (Fig. 7). The TPA molecules form dimers in which two TPA molecules form van der Waals contacts by phenyl substituents. The other two phenyl substituents of TPA form shortened van der Waals contacts with the C_{60} molecules with the C$\cdots$C distances in the 3.20–3.43 Å range and the H$\cdots$C(C_{60}) distances in the 2.69–2.85 Å range.

Nitrogen atom of TPA in **12** has planar trigonal configuration and phenyl substituents form propeller-like geometry with the corresponding torsion angles equal to 39.0(2)°, 36.1(2)° and 51.8(2)°. On average, these angles are smaller than those in neat crystals of TPA (42–56°) (27).

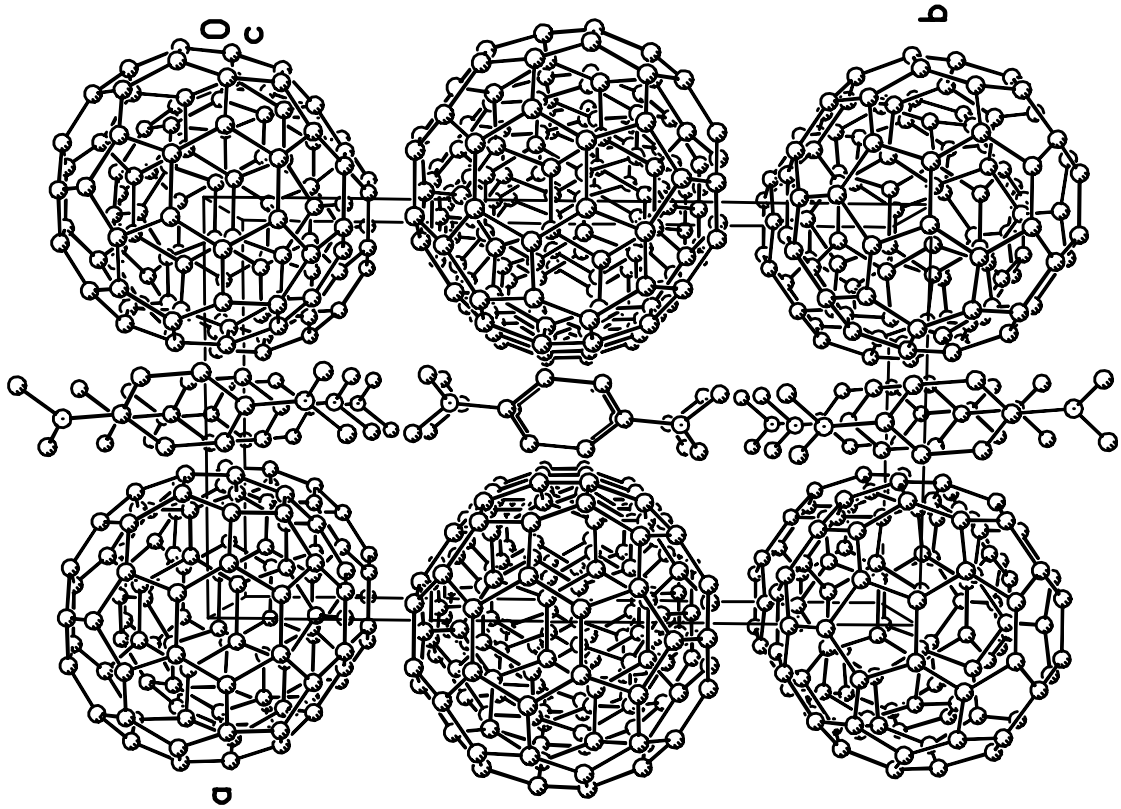

FIG. 5. The projection of crystal structure of TMPDA · C_{60} (**10**) along the *c*-axis.

The structure of all C_{60} complexes with amines is layered. The layers are strongly corrugated and form the channels in which amine molecules are located. Geometry of amine molecules in the complexes changes insignificantly probably due to their steric compliance to the fullerene sphere. The zig-zag structure of fullerene layers provides for the formation of additional van der Waals contacts between the fullerene molecules from different layers and the two-dimensional packing of C_{60} can transform to the quasi-three-dimensional one. Fullerene molecules are densely packed in the layers. The distances between the centers of C_{60} are close (**10** and **12**) to those in parent C_{60} or even shorter (**5** and **6**).

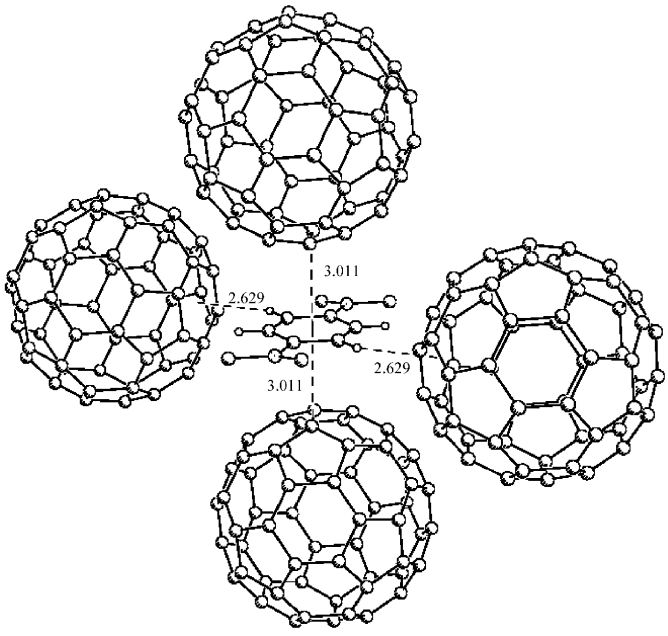

FIG. 6. The shortened van der Waals contacts between the TMPDA and C_{60} molecules in TMPDA · C_{60} (**10**) (dotted lines).

The interaction between amine and fullerene molecules is realized mainly as a result of van der Waals contacts between fullerene carbons and either phenyl or phenylene substituents of amines. The shortened N(amine)…$C(C_{60})$ van der Waals contacts are present only in **5** and **6**. The interaction between amines and C_{60} in **5**, **6**, **8**, and **10** has the π character. There are several shortened distances between the planes of the $(CH_3)_2N$–C_6H_4– fragment of the LMG molecule and C_{60} facets and relatively small dihedral angles between them (15.1° with hexagons, 21.3° with pentagons) in **5** and **6**. In **8**, the TBPDA molecules (***II***) form short van der Waals contacts by the central phenylene group with hexagons of the two C_{60} molecules with the distances in the 3.33–3.52 Å range and their parallel arrangement (the dihedral angle is 5.8°). The small distance between the centers of benzene ring of TMPDA and 6–6

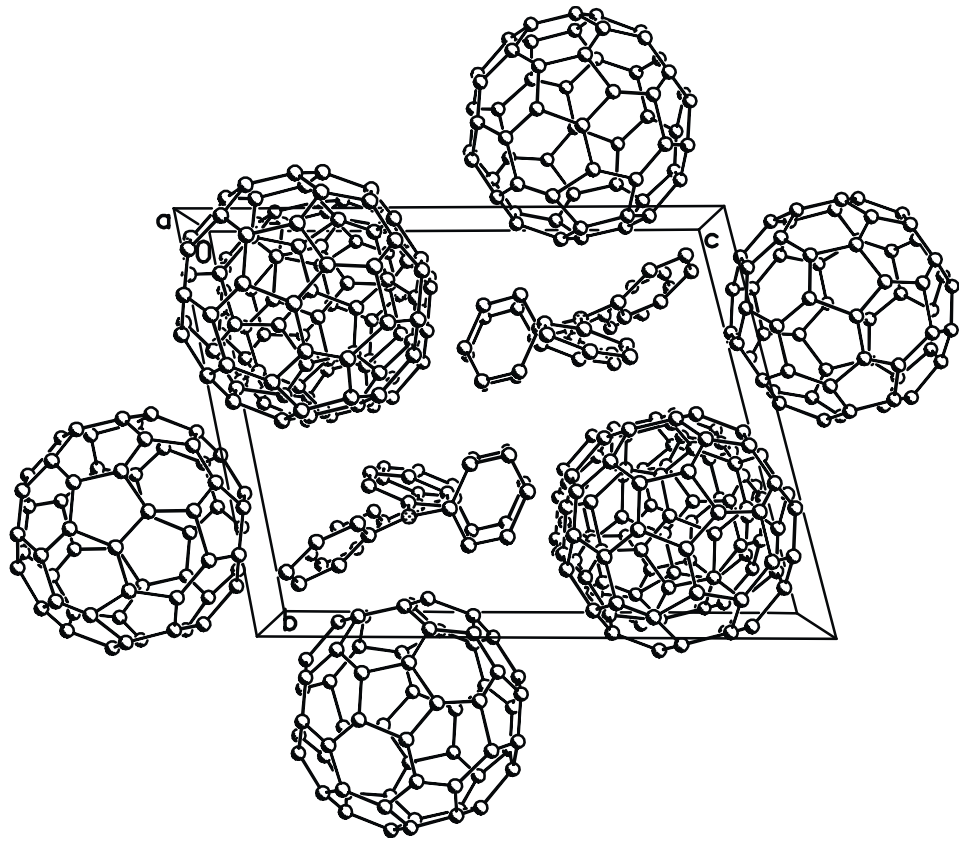

FIG. 7. The projection of crystal structure of TPA · C_{60} (**12**) along the *a*-axis.

bonds of two C_{60} molecules of 3.01 Å and the dihedral angle between them equal to 0.8° are also observed in **10**. At the same time in spite of short C···C van der Waals contacts between phenyl substituents of TPA and C_{60} facets in **12**, the overlapping of π orbitals of the TPA and C_{60} molecules is hindered due to the mutual non-parallel arrangement of these fragments.

In **5**, **10**, and **12** the interaction between amine and C_{60} molecules is weak and results in fullerene molecules disordering even at 90 K, in contrast to the C_{60} complexes with metalloporphyrins, metallocenes, and some substituted tetrathiafulvalenes (17, 23, 28). The formation of the additional naphthalene–C_{60} van der Waals contacts in 6 provides for ordered fullerene molecules. The strongest donor-acceptor interaction is realized in **10**. Probably because of steric compliance and close arrangement of the TMPDA molecules and hexagons of C_{60}, efficient interaction is possible between the π-systems of TMPDA and C_{60}. The interaction additionally intensifies due to charge transfer. All this results in the C_{60} molecules ordering in the structure of **10**.

All crystals are stable in storage except LMG · C_{60} · C_6H_6 (**4**). Probably the cavity in **4** is too large for the C_6H_6 molecules and the crystals are unstable due to the loss of solvent. Larger solvent molecules, namely, toluene (C_7H_8), and chlorobenzene (C_6H_5Cl) allow the preparation of stable crystals of LMG · C_{60} · $0.2C_7H_8$ · $0.3C_6H_5Cl$ (**5**), but with the disordered solvent and C_{60} molecules. The substitution of the solvent

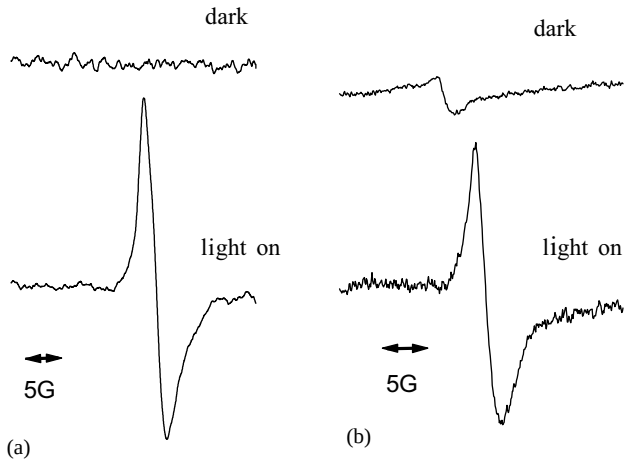

FIG. 8. The "dark" and the "light on" ESR signals at $P_{\mu\omega} = 64$ mW in (a) TMPDA · C_{60} (**10**) at 57 K and (b) LCV · C_{60} · C_6H_5Cl (**1**) at 77 K.

molecules in **4** by naphthalene ones results in the stable crystals of LMG · C_{60} · $0.5C_{10}H_8$ (**6**). Probably the size of naphthalene molecules optimally conforms to the size of the cavity and the insertion of naphthalene results in the ordering of C_{60} and naphthalene molecules in **6**. The incorporation of Cp_2Fe molecules into the positions of the solvent molecules was observed earlier in the C_{60} complexes with tetraphenylmetalloporphyrins (MTPP · Py)$_2C_{60}$ · C_7H_8 · Cp_2Fe ($M = Zn^{II}$ and Co^{II}), in which one cavity of two has the bulk shape and can accommodate Cp_2Fe molecules (29).

IR spectra for the resulting compounds appear as a superposition of those for the starting donors, corresponding amines and solvents. The shifts of the bands of the starting amines in the complexes are minor (within $6\,cm^{-1}$) and can be associated with small changes in initial geometry as a result of the formation of van der Waals contacts with fullerene spheres.

The bands of fullerenes in **1–9**, and **12–14** are not shifted relative to the starting compounds and indicate the absence of charge transfer to fullerene molecules in the resulting complexes. However, the IR spectrum of **10** manifests the shift by $3\,cm^{-1}$ of the bands of $F_{1u}(4)$ mode which is the most sensitive to charge transfer to the C_{60} molecule (30). This can be associated with certain charge transfer from TMPDA to C_{60} in the ground state. In fact, TMPDA is the strongest donor (IP = 6.2 eV (31)) among amines used. However, its "dark" ESR spectrum shows no signals attributed to the $C_{60}^{-\bullet}$ radical anion (Fig. 8).

UV–visible–NIR–spectra of the complexes contain only the bands of the fullerenes since the bands of amines are closed by more intense bands of fullerenes in the UV-range. The bands of fullerenes in the complexes somewhat shift to higher energies (up to 4 nm) relative to those of the starting ones. In the NIR-range the bands characteristic of fullerene radical anions are absent indicating the neutral ground state of the complexes.

Fullerene complexes commonly exhibit a relatively weak charge transfer band (CTB) associated with steric hindrances upon the overlapping of π-orbitals of initially planar donor molecules and the C_{60} sphere. (32, 33). However, in the spectra of the most complexes with amines (**1–7**, and **9**) intense CTBs manifest in the visible and NIR range with the maxima at: LCV (**1**)— 732, LMG (**4**)— 727; (**5**)— 737; (**6**)— 720, CVL (**7**)— 727, TBPDA (**8**)— 896 and TMPDA (**10**)— 927 nm (Fig. 9). In accordance with the X-ray analysis this may be evidence of efficient overlapping of π-orbitals of LMG, TBPDA and TMPDA and fullerene.

There are no CTBs in the optical spectra of the C_{70} complexes with LCV, TBPDA TMPDA. Probably because of different shape of the C_{60} and C_{70} molecules, the overlapping of π-orbitals of fullerene and amine is more hindered in the C_{70} complexes than in the C_{60} ones. In contrast to TMPDA · C_{60}, the IR spectrum of TMPDA · C_{70} does not manifest any shifts of the bands attributed to C_{70} (within $\pm 1\,cm^{-1}$).

Photoexcitation of the Complexes. LESR-Spectra

The "dark" ESR signals attributed to $C_{60}^{-\bullet}$ (34, 35) are absent in **1–15**. In some cases, the "dark" ESR spectra contain narrow weak ESR signals with $g = 2.0022$ and $\Delta H = 1.5$–2 G (Fig. 8b) attributed to defects which appear due to the interaction of fullerenes with oxygen (36) or $C_{120}O$ impurities (39).

According to the IR- and UV–visible–NIR-spectra, the resulting complexes have a neutral ground state. Photoexcitation of the neutral complexes can result in the excited ionic state with charge separation: $D^{+\delta}\,A^{-\delta} \rightarrow D^{+(1-\delta)}\,A^{-(1-\delta)}$, where δ is close to 0(**I**)

We studied PIET in complexes **1** and **10** by LESR spectroscopy (9). Photoexcitation of the complexes was carried out using white light (400–900 nm) at 100 K. At photoexcitation of **1** and **10**, the LESR signals with $g = 1.9984$–1.9992 and $\Delta H = 3.9$–4.2 G appeared (Fig. 8). The signals were not saturated until highest available microwave power (200 mW) and disappeared below 20 μW microwave power. It is known (35, 36) that the ESR signal of the $C_{60}^{-\bullet}$ radical anion (35, 36) has g-factor of 1.996–2.000 with ΔH 20–50 G at room temperature and is narrowed to 4–10 G with the temperature decrease down to 77 K The LESR signals observed in **1** and **10** have the same parameters at 100 K and, therefore, can be attributed to the $C_{60}^{-\bullet}$ radical anions (9).

The dependencies of the LESR signal intensity on the photon energy for **1** and **10** are shown in Fig. 10. It is seen

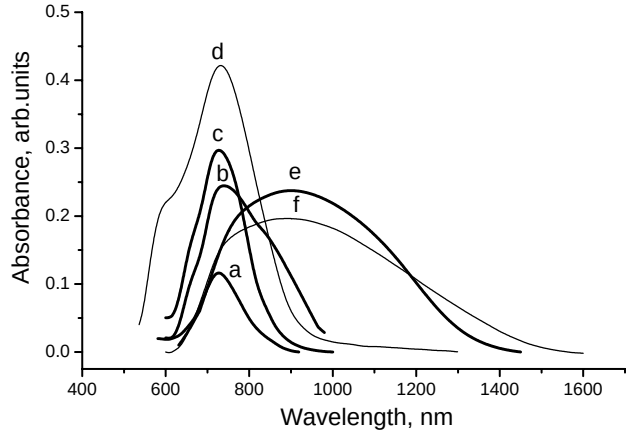

FIG. 9. Charge transfer bands discriminated from the optical absorption spectra of: (a) CVL · C_{60} · C_6H_6 (**7**); (b) LMG · C_{60} · $0.2C_7H_8$ · $0.3C_6H_5Cl$ (**5**); (c) LMG · C_{60} · C_6H_6 (**4**); (d) LCV · C_{60} · C_6H_5Cl (**1**); (e) TBPDA$(C_{60})_2$ (**8**); and (f) TMPDA · C_{60} (**10**) by a subtraction of normalized spectrum of C_{60} from that of the complex.

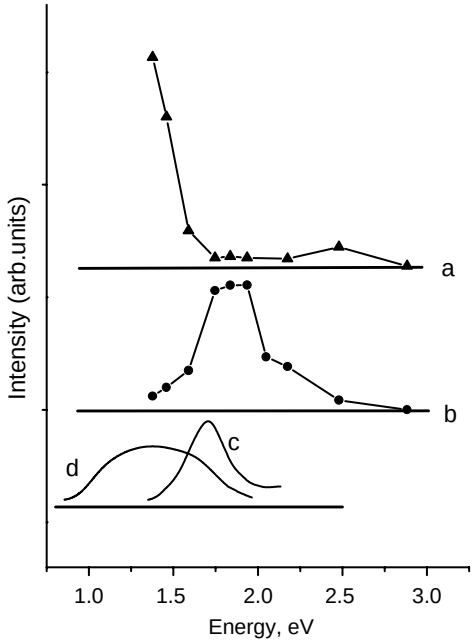

FIG. 10. The dependence of LESR signal intensity on photon energy: (a) LCV · C_{60} · C_6H_5Cl (**1**) and (b) TMPDA · C_{60} (**10**). The CTBs were discriminated from the absorption spectra of (c) LCV · C_{60} · C_6H_5Cl (**1**) and TMPDA · C_{60} (**10**) for comparison.

that all the peaks lie at energies less than 2.25 eV though the positions of the maxima for these peaks are different. The maximum for **10** is located in the 2.25–1.65 eV range (Fig. 10 b), whereas the maximum for 1 lies at energies lower than 1.46 eV (Fig. 10 a).

Different mechanisms are possible for the generation of the LESR signals from the $C_{60}^{-\bullet}$ radical anions under photoexcitation of fullerene complexes with amines by white light in the 400–900 nm range (Fig. 11):

Photoexcitation of the donor component (Fig. 11a_1) is followed by electron transfer to the C_{60} molecule (Fig. 11a_2). However, photoexcitation of amines used in this work is possible only in the UV-range.

Since the C_{60} molecule is a stronger acceptor in the excited than in the ground state (38), photoexcitation of C_{60} (Fig. 11b_1) can also result in electron transfer from the donor to the excited C_{60} molecule (Fig. 11b_2). Due to that the direct HOMO–LUMO transitions are symmetry forbidden in the C_{60} and have very low intensity (39), photoexcitation of C_{60} is realized mainly at energies higher than 2 eV.

Direct intermolecular charge transfer from the donor to the C_{60} molecule (Fig. 11c) is also possible. As it was mentioned above, CTBs in the complexes under study are observed at 1–2 eV in the Vis–NIR-range.

The LESR signals were observed under photoexcitation of the complexes with the photon energy lower than 2.25 eV. Because of this, the PIET mechanism can be

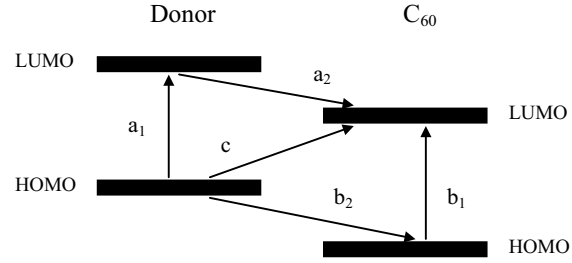

FIG. 11. The diagram of possible mechanisms of PIET in the C_{60} complexes with amines: (a) excitation of the donor component; (b) excitation of C_{60} followed by electron transfer from donor to excited C_{60}; (c) direct charge transfer from donor to C_{60}.

attributed mainly to intermolecular charge transfer from the donor to the C_{60} molecule.

CONCLUSION

New molecular complexes of C_{60} and C_{70} with different amines have been prepared. Crystal structures of the C_{60} complexes with LMG, TMPDA, TBPDA and TPA have been solved. It has been shown that **5, 6,** and **10** have a layered packing of the C_{60} molecules, while **8** and **12** have a quasi-three-dimensional packing due to the distortion of the layers.

Insertion of molecules of different size into cavities of the complex is possible. Insertion of small solvent molecules results in unstable crystals (**4**), insertion of larger ones results in stable crystals (**5**) with disordered both C_{60} and solvent molecules, while insertion of the largest naphthalene molecules results in the stable crystals (**6**) with fully ordered molecules. The complexes with such large cavities give the opportunity to the development of multi-component complexes by incorporation of different donor molecules into the cavity (29).

According to the data of IR-, UV–visible–NIR-, and ESR-spectroscopy the compounds obtained have a neutral ground state. The spectra of **1–8**, and **10** show the intense CTBs in visible and NIR-range. The presence of these bands allows these compounds to be attributed to charge transfer complexes. At photoexcitation of **1** and **10** by white light in the 400–900 nm range, the LESR signals attributed to the $C_{60}^{-\bullet}$ radical anions were observed at 100 K. The range of light energies (<2.25 eV) in which the LESR signals were produced shows that photoinduced electron transfer is realized mainly by direct charge transfer from amine to the C_{60} molecule.

ACKNOWLEDGMENTS

The work was supported by the Linkage Grant of NATO Science Program, Russian Program "Fullerenes and Atomic Clusters," Russian

Foundation for Basic Research (Grant 00-03-32577a) and National Science Foundation (CHE9981864).

REFERENCES

1. M. J. Rosseinsky, *J. Mater. Chem.* **5,** 1497 (1995).
2. P. W. Stephens, D. Cox, J. W. Lauher, L. Mihaly, J. B. Wiley, P.-M. Allemand, A. Hirsch, K. Holczer, Q. Li, J. D. Thompson, and F. Wudl, *Nature (London)* **355,** 331 (1992).
3. D. V. Konarev and R. N. Lyubovskaya, *Russ. Chem. Rev.* **68,** 19 (1999).
4. N. S. Sariciftci and A. J. Heeger, *in* "Handbook of Organic Conductive Molecules and Polymers," (H. S. Nalwa, Ed.), Vol. 1, p. 414. John Wiley and Sons Ltd., New York 1997.
5. D. M. Guldi, *Chem. Commun.* 321 (2000).
6. N. Martin, L. Sanchez, B. Illescas, and I. Perez, *Chem. Rev.* **198,** 2527 (1998).
7. F. D'Souza, G. R. Deviprasad, M. S. Rahman, and J.-P. Choi, *Inorg. Chem.* **38,** 2157 (1999).
8. F. D'Souza, N. P. Rath, G. R. Deviprasad, and M. E. Zandler, *Chem. Commun.* 267 (2001).
9. D. V. Konarev, G. Zerza, M. Sharber, N. S. Sariciftci, and R. N. Lyubovskaya, *Synth. Met.* **121,** 1127 (2001).
10. R. J. Sension, A. Z. Szarka, G. R. Smith, and R. M. Hochstrasser, *Chem. Phys. Lett.* **185,** 179 (1991).
11. V. A. Nadtochenko, N. N. Denisov, and P. P. Levin, *Izv. Acad. Nauk. Ser. Khim.* **44,** 1078 (1995). (in Russian)
12. V. A. Nadtochenko, N. N. Denisov, I. V. Rubtsov, and A. P. Moravskii, *Izv. Akad. Nauk. Ser. Khim.* **45,** 1151 (1996). (in Russian)
13. S. P. Sibley, R. L. Campbell, and H. B. Silber, *J. Phys. Chem.* **99,** 5274 (1995).
14. Schider, B. Gotschy, A. Seidl, and R. Gompper, *Chem. Phys.* **193,** 321 (1995).
15. D. M. Eichhorn, S. Yang, W. Jarrell, T. F. Baumann, L. S. Beall, A. J. P. White, D. J. Williams, A. G. M. Barrett, and B. M. Hoffman, *Chem. Commun.* 1703 (1995).
16. P. D. W. Boyd, M. C. Hodgson, C. E. F. Rickard, A. G. Oliver, L. Chaker, P. J. Brothers, R. D. Bolskar, F. S. Tham, and C. A. Reed, *J. Am. Chem. Soc.* **121,** 10487 (1999).
17. D. V. Konarev, I. S. Neretin, Yu. L. Slovokhotov, E. I. Yudanova, N. V. Drichko, Yu. M. Shul'ga, B. P. Tarasov, L. L. Gumanov, A. S. Batsanov, J. A. K. Howard, and R. N. Lyubovskaya, *Chem. Eur. J.* **7,** 2605 (2001).
18. V. A. Nadtochenko, A. P. Moravskii, V. V. Gritsenko, G. V. Shilov, and O. A. D'yachenko, *Mol. Cryst. Liq. Cryst. Sci. Technol. Sect. C* **7,** 103 (1996).
19. E. M. Veen, P. M. Postma, H. T. Jonkman, A. L. Spek, and B. L. Feringa, *Chem. Commun.* 1709 (1999).
20. A. L. Litvinov, D. V. Konarev, R. N. Lyubovskaya, B. P. Tarasov, I. S. Neretin, and Yu. L. Slovokhotov, *Synth. Met.* **121,** 1125 (2001).
21. SMART and SAINT, "Area Detector Control and Integration Software, Ver. 6.01." Bruker Analytical X-ray Systems, Madison, WI, USA, 1999.
22. SHELXTL, "An Integrated System for Solving, Refining and Displaying Crystal Structures from Diffraction Data, Ver. 5.10." Bruker Analytical X-ray Systems, Madison, WI, USA, 1997.
23. D. V. Konarev, R. N. Lyubovskaya, N. V. Drichko, E. I. Yudanova, Yu. M. Shul'ga, A. L. Litvinov, V. N. Semkin, and B. P. Tarasov, *J. Mater. Chem.* **10,** 803 (2000).
24. H.-B. Burgi, E. Blanc, D. Schwarzenbach, Shengzhong Liu, Ying-jie Lu, M. M. Kappes, and J. A. Ibers. *Angew. Chem. Int. Ed. Engl.* **31,** 640 (1992).
25. P. W. Stephens, G. Bortel, G. Faigel, M. Tegze, A. Janossy, S. Pekker, G. Oszlanyi, and L. Forro, *Nature* **370,** 636 (1994).
26. C. Richert, M. Pirotta, and T. Muller, *Acta Crystallogr. C* **48,** 2233 (1992).
27. A. N. Sobolev, V. K. Bel'skiy, I. P. Romm, N. Yu. Chernikova, and E. N. Guryanova, *Acta Crystallogr. C* **41,** 967 (1995).
28. Izuoka, T. Tachikawa, T. Sugawara, Y. Suzuki, M. Konno, Y. Saito, and H. Shinohara, *Chem. Commun.* 1472 (1992).
29. D. V. Konarev, A. Yu. Kovalevsky, X. Li, I. S. Neretin, A. L. Litvinov, N. V. Drichko, Y. L. Slovokhotov, P. Coppens, and R. N. Lyubovskaya, *Inorg. Chem.* **41,** 3638 (2002).
30. T. Picher, R. Winkler, and H. Kuzmany, *Phys. Rev. B* **49,** 15879 (1994).
31. R. Egdell, J. C. Green, and C. N. R. Rao, *Chem. Phys. Lett.* **33,** 600 (1975).
32. D. V. Konarev, V. N. Semkin, A. Graja, and R. N. Lyubovskaya, *J. Mol. Struct.* **450,** 11 (1998).
33. D. V. Konarev, R. N. Lyubovskaya, N. V. Drichko, V. N. Semkin, and A. Graja. *Chem. Phys. Lett.* **314,** 570 (1999).
34. A. J. Schell-Sorokin, F. Mehran, G. R. Eaton, S. S. Eaton, A. Viehbeck, T. R. O'Toole, and C. A. Brown, *Chem. Phys. Lett.* **195,** 225 (1992).
35. J. Stinchcombe, A. Penicaud, P. Bhyrappa, P. D. W. Boyd, and C. A. Reed, *J. Am. Chem. Soc.* **115,** 5212 (1993).
36. M. D. Pace, T. C. Christidis, J. J. Yin, and J. Millikin, *Phys. Chem.* **96,** 6858 (1992).
37. P. Paul, R. D. Bolskar, A. M. Clark, and C. A. Reed, *Chem. Commun.* 1229 (2000).
38. G. P. Zhang, R. T. Fu, X. Sun, X. F. Zong, K. H. Lee, and T. Y. Park, *J. Phys. Chem.* **99,** 12301 (1995).
39. M. S. Dresselhaus, G. Dresselhaus, and P. C. Eklund, "Science of Fullerenes and Carbon Nanotubes."AcademicPress, San Diego, 1996.